Acene adsorption on a Fibonacci-modulated Cu film

K. M. Young[1], J. A. Smerdon[1], H. R. Sharma[1], M. Lahti[2], K. Pussi[2], and R. McGrath[1]

[1]*Department of Physics, University of Liverpool, Oxford Street, L69 7ZE UK and*

[2]*Department of Mathematics and Physics,*

Lappeenranta University of Technology, PO Box 20, FIN-53851 Finland

(Dated: January 7, 2013)

Abstract

The adsorption of pentacene (Pn) on the 5-fold surface of the *i*-Al-Pd-Mn quasicrystal and on the one-dimensionally aperiodic Cu multi-layer formed thereon has been observed with scanning tunneling microscopy. The molecule has a strong interaction with the clean quasicrystal surface leading to the formation of a disordered layer. On the Cu film, a molecular layer assembles with the Cu rows acting as a template. At lower coverages, there is a repulsive interaction between the molecules leading to a dispersed homogeneous arrangement. At higher coverages, the steric interaction of the Pn molecules counterbalances the aperiodic template which results in a short-range periodic 'checkerboard' arrangement of molecules. DFT calculations using lower-order acenes have been used to probe the details of the interactions with the aperiodic Cu surface and it is found that adsorption with molecules parallel to Cu rows is preferred, in agreement with experimental results.

I. INTRODUCTION

Quasicrystals are metallic alloys that exhibit long range ordering but with the absence of translational periodicity[1]. Their aperiodic structure has high orders of symmetry which cannot be described using a Bravais lattice. The complex surfaces of quasicrystals offer a variety of adsorption sites and an aperiodic template to enforce order on incident atoms or molecules. In addition to providing an interesting substrate to study the fundamentals of epitaxial growth, there is great attraction in the possibility of growing aperiodic layers of single elements and thus distinguishing the effects of the quasicrystalline ordering of such layers from the chemical complexity inherent in alloy surfaces. Consequently there has been extensive research on growth at quasicrystal surfaces, mostly involving metals. To date various atomic epitaxial systems have been found[2–4].

It is of interest to determine whether larger entities such as molecules can be induced to mimic quasicrystalline order upon deposition. There have been numerous theoretical and experimental studies of potential candidates for the formation of molecular aperiodic films[5–11], but growth displaying extended quasiperiodic ordering has not been found experimentally.

Cu exhibits almost layer-by-layer growth on the 5-fold surface of Al-Pd-Mn; subsequent layers start to form when the underlying layer is around 60% completed[12]. An ordered, one-dimensionally pseudomorphic Cu multilayer is formed at coverages above ∼4 monolayer (ML). It is composed of epitaxially oriented domains which are commensurate with the quasicrystalline substrate in one dimension. The aperiodic domains of Cu were first observed experimentally with scanning tunneling microscopy (STM) and low-energy electron diffraction (LEED)[13]. An aperiodic sequence of two different sized rows was measured, with short (S =0.46 ± 0.02 nm) and long (L =0.74 ± 0.02 nm) spacings. Using dynamical LEED this structure was found to be a vicinal surface of a body-centered tetragonal bct-(100) Cu structure[14], with the Cu steps at the quasicrystal/Cu interface being commensurate with characteristic distances on the quasicrystal surface.

Pentacene ($C_{22}H_{14}$, dimensions 1.42 nm × 0.5 nm, Pn) is a *p*-type organic semiconductor consisting of five linearly bonded benzene rings. It is primarily of interest in thin film formation as it has a tendency to form flat, ordered layers on metallic surfaces[15–19]. The ordered, layer-by-layer growth of Pn and its desirable electronic properties have led to intense research aimed at incorporating Pn films as part of the active layer in organic semiconductor

devices, such as photovoltaic cells and organic field effect transistors (OFETs). Performance for such devices to date exceeds that of amorphous silicon, with a reported charge mobility of 1 cm^2/Vs[20]. It has been suggested that understanding the growth of Pn at surfaces – including interface effects and to extend the range of film order – is essential to improve device performance[21].

Adsorption of aromatic molecules on Pt and other *d*-band metal surfaces to investigate the interaction between surface electronic structure and the band structure of the molecule has been well studied[22–26]. The interaction between the *d*-band of the metal surface and the π system of the molecule leads to well defined adsorption sites for every C atom in the molecule[23,24]. In previous studies it has been found that some distortion of the molecule and surface affects the adsorption energy: large distortions cost energy but can lead to larger adsorption energies between the surface and the molecule[27]. The distortion energy of the aromatic molecule is linked to the C-C bond length and bond angles.

This article reports the experimental investigation with scanning tunneling microscopy (STM) of the sub-monolayer growth of Pn on the fivefold surface of the *i*-Al-Pd-Mn quasicrystal and on the one-dimensionally aperiodic Cu multilayer pre-deposited on this substrate. Additionally, the interactions between naphthalene and anthracene and the aperiodic Cu film have been investigated using density functional theory (DFT). In previous studies it has been found that in the case of a smooth surface the electronic interaction between a polycyclic molecule with a given number of acene rings and the surface is similar to the sum of the interaction of the same number of acene rings provided by monocyclic benzene molecules and the surface[23,24]. Therefore it is possible to identify the trend for pentacene adsorption by studying the adsorption of naphthalene and anthracene, with the caveat that an aperiodic Cu surface allows many more possible adsorption sites than smooth Cu(111). The non-close-packed surface structure of the Fibonacci-modulated Cu also offers a much greater potential for surface distortions and richer interactions with the molecules, through the lower coordination of surface Cu atoms.

II. EXPERIMENTAL DETAILS

A variable temperature Omicron STM (VT-STM) was used for collection of STM data. Tips were electrochemically etched from W wire and thoroughly rinsed with water before

introduction to the chamber. Base pressure during scanning was 1.2×10^{-10} mbar. The sample was at room temperature throughout the experiment.

The sample was grown via the Czochralski technique with a nominal composition of $Al_{70}Pd_{21}Mn_9$ and cut perpendicular to a 5-fold axis. It was prepared in ultra-high-vacuum (UHV) by cycles of sputtering (2 keV Ar^+ ions for 30 minutes) and annealing (2 hours at 920 K). This method of surface preparation has been shown to yield a step and terrace morphology equivalent to a bulk truncation with a small amount of inter-layer relaxation[28]. The quasicrystalline order at the surface was checked after preparation using STM. A distinct 10-fold fast Fourier transform (FFT) was obtained from images of flat terraces. The source of such order is truncated bulk clusters which form surface features termed "dark stars" and "white flowers"[29].

Pentacene was evaporated from a Pyrex tube with a tungsten filament tightly wrapped around it. The evaporator was repeatedly degassed to an operating temperature of 393 ± 2 K, as measured by a K type thermocouple. A 10 second deposition with a thermocouple temperature 393 K resulted in a coverage of 0.17 ± 0.04 ML, determined by thresholding STM data collected in the sub-monolayer regime. One monolayer is defined as a layer of adsorbate that completely covers the substrate. Cu was evaporated from a simple filament source consisting of a piece of OFHC Cu wrapped with a W filament. The formation of the Cu multilayer structure was monitored with STM.

III. RESULTS AND ANALYSIS

A. Pn adsorption on the 5-fold AlPdMn quasicrystal surface

Figure 1 a-c) show STM images following deposition of Pn on the 5-fold Al-Pd-Mn surface. The Pn molecules appear as elongated protrusions and the substrate features are imaged simultaneously. The size of the small dark holes from the substrate corresponds to the "dark star" features observed previously[29]. The molecules are evenly distributed across the surface and no local clustering is observed.

The molecules exhibit increased tunneling current at either end for the range of bias voltages ±1.8 V. This charge-density distribution has been observed in other studies[18,22]. A line profile parallel to the long axis of the molecule is displayed in the inset to Figure 1

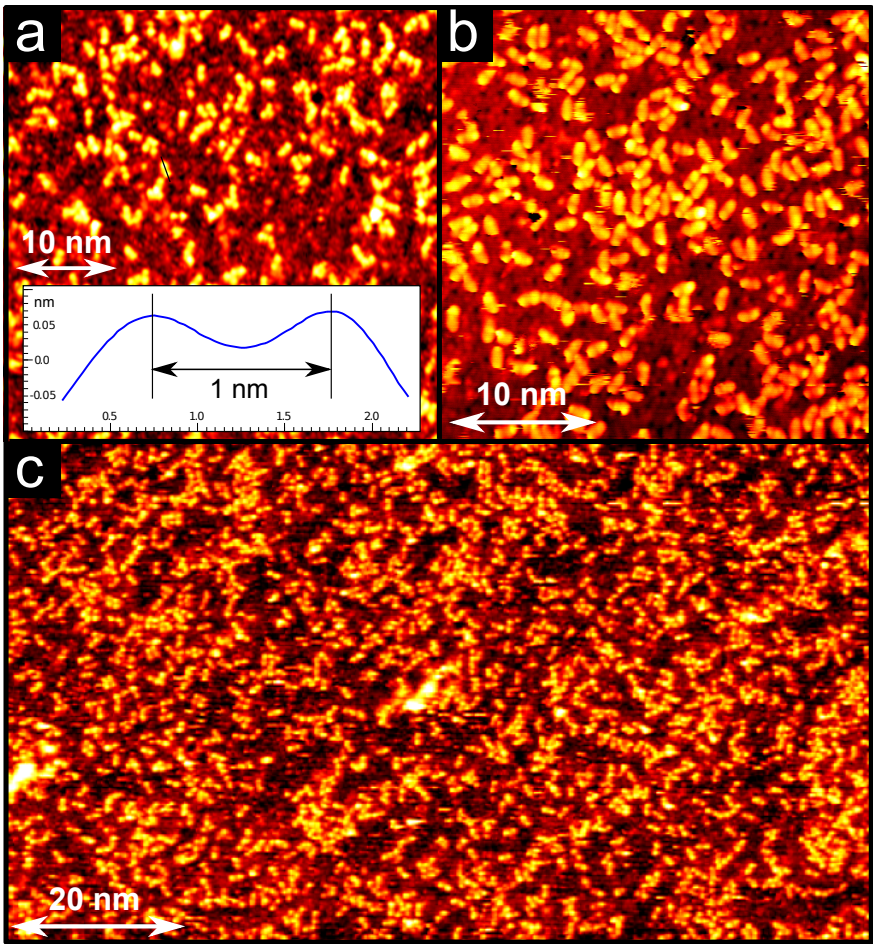

FIG. 1. a) 50 nm × 50 nm STM image of 0.17 ± 0.04 ML of Pn deposited on clean *i*-Al-Pd-Mn ($V_{sample} = -1.1$ V, I = 0.1 nA) *Inset*: Profile along the molecular axis of a Pn molecule showing the peak-to-peak length. b) 30 nm × 30 nm, 0.22 ML, ($V_{sample} = 1.8$ V, I = 0.1 nA) c) 100 nm × 57 nm, 0.22 ML, ($V_{sample} = 1.0$ V, I = 0.1 nA)

a). The distance of 1.0 nm measured between the maxima in tip height is approximately equal to the spacing of the outer benzene rings in an isolated Pn molecule. The dimensions indicate that the features are single molecules adsorbed intact with their long molecular axis parallel to the surface. For the range of tunneling conditions used the molecule surfaces lay in the range of z-positions 0.08–0.2 nm above the substrate surface, which leads to the conclusion that the molecular plane is parallel to the surface.

The Pn film has no particular quasiperiodic ordering. After thresholding the image to generate a binary image with Pn bright and substrate dark, autocorrelation functions and FFTs show that no ordering can be detected in the molecular positions. This, coupled with

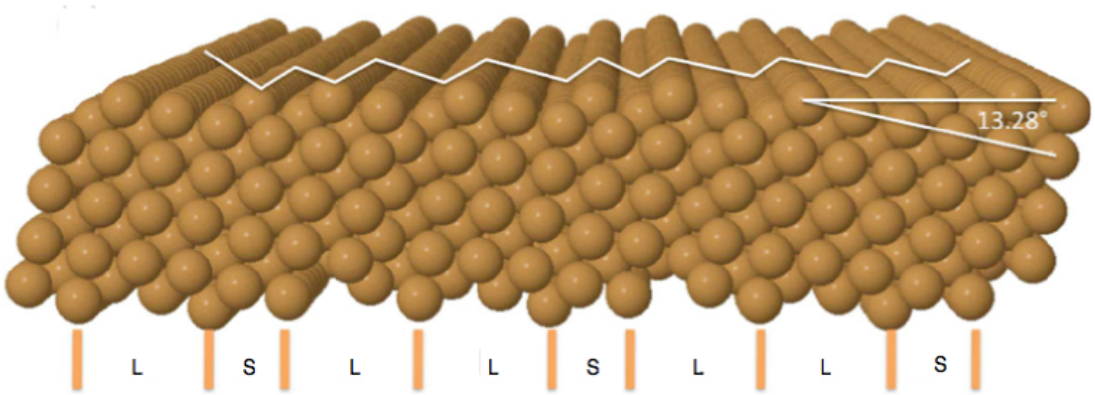

FIG. 2. The body-centred tetragonal Cu domain structure as elucidated via dynamical LEED. Reprinted from reference[14].

the homogeneous distribution of molecules observed in Fig 1(c), indicates that molecules stick where they impinge on the surface and do not diffuse to find quasiperiodically arranged sites.

B. Growth of Pn on the one-dimensionally aperiodic Cu multilayer

The Cu film follows the Franke-van der Merwe (layer-by-layer) growth mode, with the caveat that the next layer begins to form when the preceding layer is approximately 60% complete. This ultimately results in pyramidal structures at high coverages[12], but the coverage in the present study is similar to that in the original report[13] at approximately 4 ML, at which point the film is quite flat. Between steps, the film is very flat, with no surface modulation other than the previously described row structure.

The body-centred tetragonal (bct) Cu structure is represented in Figure 2. As the structure of the Cu film is based on step edges forming an aperiodic sequence commensurate with the underlying quasicrystal, the surface is vicinal[14]. However, the step height (or row modulation) here is small, of the order of 0.7 Å, so the 'steps' are imaged as linear features in a flat film, rather than as a pattern of ridges and valleys.

When deposited on this film, Pn molecules are homogeneously dispersed, except for portions of the film which remain uncovered. These regions are strictly delineated and follow features of the Cu film such as domain boundaries. This behaviour was not observed in the only other study of molecules atop this film, in which C_{60} molecules randomly decorate

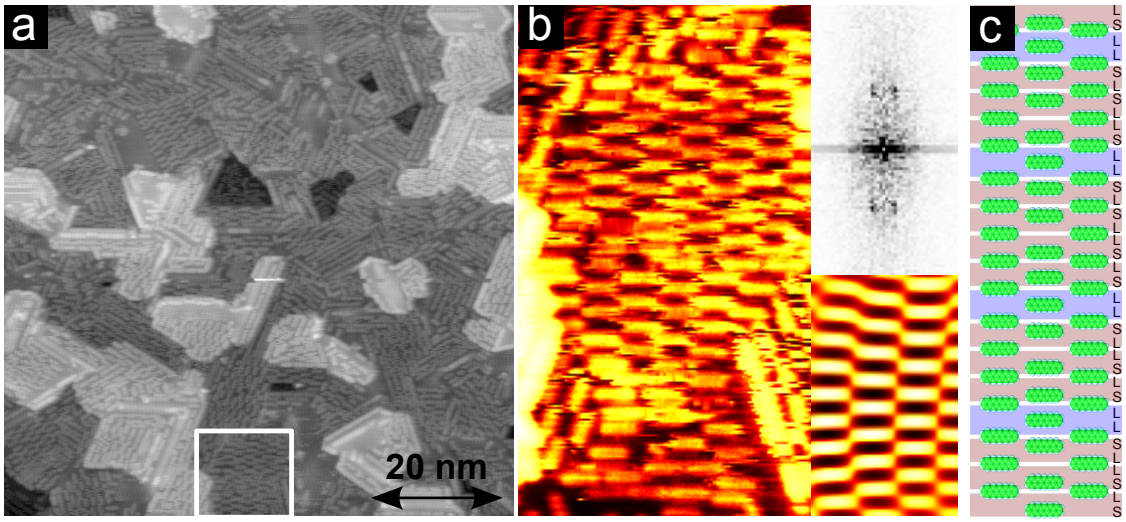

FIG. 3. (a) $(3.62 \pm 0.5) \times 10^{13}$ molecules/cm^2, $V_{sample} = 1.15$ V, $I = 0.1$ nA. (b): 12 nm $\times$ 20 nm STM topograph of the Pn/Cu/AlPdMn film taken at the location indicated in (a), showing the checkerboard pattern with Fast Fourier transform of the topograph and the inverse FFT of the four clear peaks. (c) Demonstration of how the checkerboard pattern might occur based on the Fibonacci sequence. Discussion in text.

the entire film[8]. As coverage increases, the average separation of Pn molecules decreases, but islands are not formed. Instead, a homogeneous dispersion is maintained, with the uncovered regions shrinking at higher coverages. Coverages above 1 ML were not investigated as part of this study.

1. Pn 'checkerboard' structure

The Cu row structure, depicted in Figure 2 is very dense (L=7.3 Å, S=4.5 Å)[13,14]. This row separation is smaller than that of Pn molecules closely packed on a surface[18]. Therefore, each adjacent row cannot be decorated by an unbroken chain of molecules. At lower coverages, some chain features are observed, but at higher coverages, a 'checkerboard' structure is observed, shown in Figure 3(a,b).

This checkerboard structure appears largely periodic. The molecule separation perpendicular to the molecular long axis in any single domain is on average 11.3 ± 1 Å, (measured from several rotational domains in order to minimise systematic error due to skew).

By considering the underlying Cu row structure, we can determine that the sum of the

row separations of indistinguishable LS or SL motifs is $7.3 + 4.5 = 11.8$ Å. If adjacent terms in a binary Fibonacci sequence of two lengths L and S are added together, LS becomes indistinguishable from SL and gives a pattern with much longer periodic sequences than exist in the original sequence. The new sequence looks like that depicted by the blue and pink rows in Figure 3(c). This suggests a model to explain the checkerboard structure. From the figure, it is clear that even this simple modification of the aperiodic sequence results in periodic-like Pn domains, with a separation consistent with that expected. The Pn molecules on the right and left of the diagram follow this sequence. In the centre, the molecules decorate the closest row of the original Fibonacci sequence, which similarly gives a sequence with long periodic sequences that extend to 4 or 5 molecules. As the molecules can get closer together parallel to their long axes, this provides better packing than chains separated by two LS/SL or LL segments.

2. Modification of LDOS of Cu film

Figure 4 shows the Pn/Cu/Al-Pd-Mn film at a submonolayer coverage of $(2.04 \pm 0.08) \times 10^{13}$ molecules/cm^2. The plane-subtracted data are presented without any processing in order to prevent obscuration of finer details of the image. The noise apparent around certain molecules can be interpreted as evidence that the molecules are somewhat mobile under these conditions[18]. Mobile species on a surface usually form islands[9,30] via an attractive interaction. The molecular mobility and lack of islanding at any coverage studied, indicates that there is some medium-range repulsive interaction between Pn molecules that contributes to the maintenance of a homogeneous dispersion at all coverages, similarly to the case for Pn/Cu(110)[31].

The obvious question is what is the source of this repulsive interaction. When Pn molecules are deposited on Cu(110), they orient into long side-to-side chains of molecules. This ordering was found to occur simultaneously with the formation of a standing charge density wave on the Cu(110) surface, aligned along the $[1\bar{1}0]$ direction[31]. This effect, associated with the Friedel oscillations of surface state electrons, points to a periodic modulation which is not evident in the study under discussion. An alternative mechanism is the generation of a dipole in the adsorbed molecules, originating in significant charge transfer between the molecules and the substrate and leading to electrostatic repulsion between

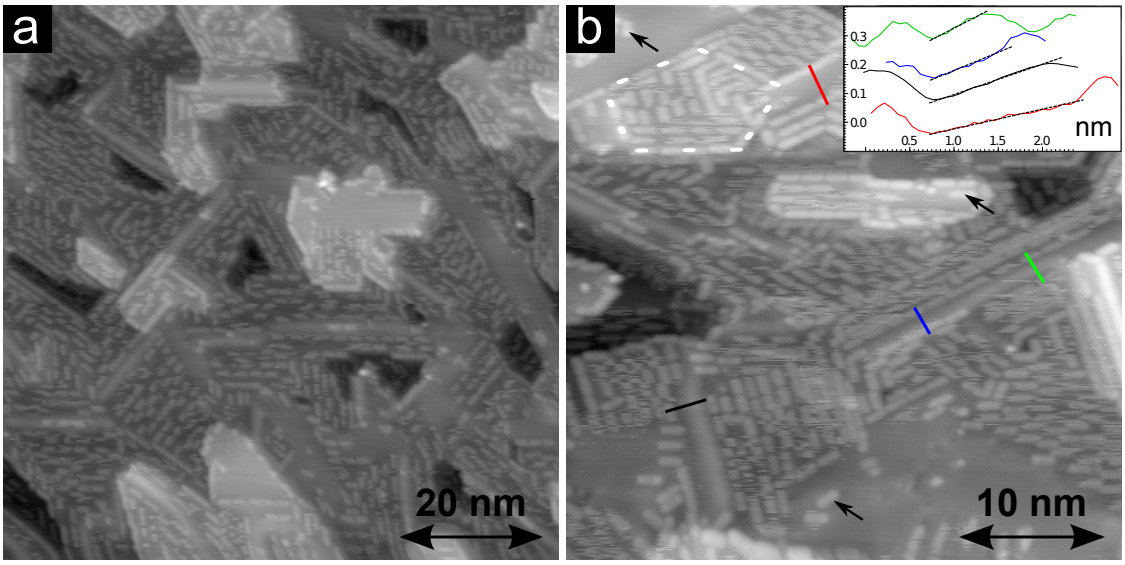

FIG. 4. (a) 80 nm × 80 nm STM topograph of the Pn/Cu/AlPdMn film at a coverage of (2.04 ± 0.08) × 10^{13} molecules/cm^2, V_{sample} = 1.03 V, I = 0.1 nA. Apart from plane-levelling, the data are unprocessed (b) 40 nm × 40 nm image at a similar coverage. There is some drift in the data, which is why the pentagon containing Pn molecules in the upper left is distorted. Inset: profiles taken along the indicated lines, showing increasing surface charge distortion as the area of exposed Cu narrows. Dashed fit lines of the gradient are superimposed. The profiles are averaged across 6 adjacent pixel lines. Some molecules which appear to affect the surface charge density of the Cu less than others are indicated with black arrows.

adsorbed molecules. This phenomenon has been observed for another electron-donating species, tetrathiafulvalene, when deposited on Au(111)[32]. The charge transfer in that study was quantified using DFT and was found to be on the order of 0.6e per molecule.

This modification of the surface charge density and the associated modification of the substrate work function ϕ is argued to be one of the main mechanisms by which molecular STM contrast originates[33]. There is evidence for this modification of the surface charge density in Figure 4(b).

The surface charge density is proportional to the conductance and variations thereof can thus be measured as variations in surface topography. The gradients of the line profiles plotted in Figure 4(b) therefore show a pronounced asymmetry in the charge distortion around Pn molecules. Knowledge of the underlying film structure allows us to observe that asymmetry is also evident in the out-of-plane tilt from (100) to approximately (7 0 30) of the

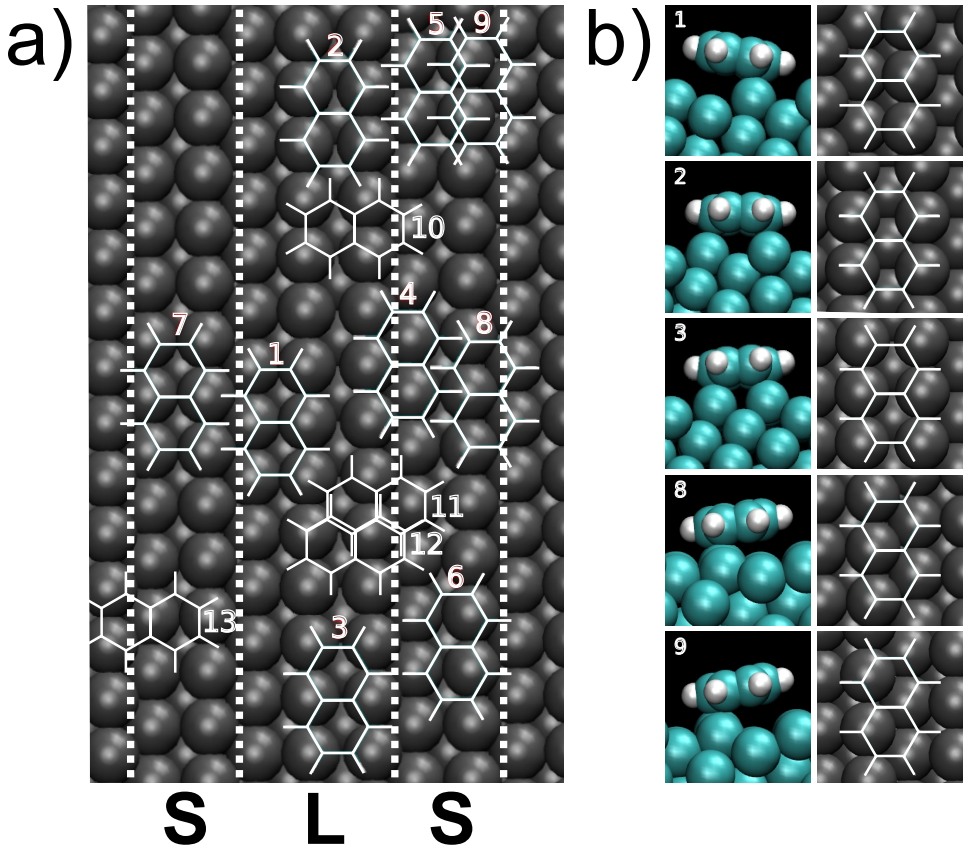

FIG. 5. (a) Adsorption sites for the naphthalene/Cu calculation adsorption parallel to Cu rows. Dotted lines are indications of the Fibonacci step structure of the Cu. (b) Side and top views of some of the relaxed adsorption configurations.

bct Cu domains – the tilt angle is not a multiple of $\pi/2$ and so the tilt operation does not result in an azimuthally symmetrical film. Therefore, the phenomena are likely to be related, and as across a complete film symmetrical tilts would produce symmetrical distortions, this is expected to be a local *symmetry breaking* phenomenon.

C. DFT calculations for acenes on Cu/AlPdMn

Density functional theory (DFT) calculations were used to aid in understanding the interaction of Pn with the vicinal Cu surface and to determine possible adsorption sites. The Vienna *ab initio* simulation package (VASP)[34,35] with the projector augmented wave (PAW)[36] potentials was employed. The generalized gradient approximation (GGA) of the Perdew-Wang 91 (PW91)[37] type was used for the exchange correlation potential. An $8\times8\times1$

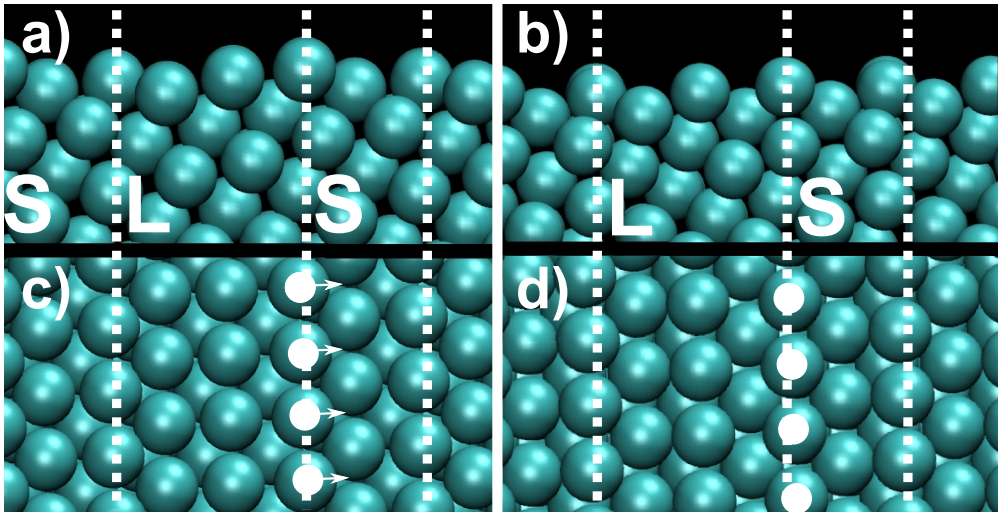

FIG. 6. (a,c) show top and side views of the undistorted relaxed substrate. (b,d) show top and side views of the distorted Cu substrate with a naphthalene molecule (not shown) located at adsorption site 9. A row of atoms that shifts significantly is indicated with white dots.

Monkhorst-Pack mesh was used for k-point sampling for naphthalene adsorption and anthracene adsorption parallel to Cu rows, and $6 \times 10 \times 1$ for anthracene adsorption perpendicular to Cu rows. The Cu surface was modeled using the supercell approach with periodic boundary conditions. The Cu supercell contained 115 atoms in 5 layers for naphthalene adsorption, 138 atoms for anthracene adsorption parallel to Cu rows and 184 atoms for anthracene adsorption perpendicular to Cu rows. The model included a 2.2 nm vacuum layer. During geometry relaxation the lowest Cu layer was fixed. The naphthalene molecule – an acene with two benzene rings – was used instead of Pn to reduce calculation times. The molecule was placed at different potential adsorption sites along the rows. Adsorption energies were then calculated, defined as $E_{ads} = E_{tot} - E_{clean} - E_{mol}$, where E_{tot} is the total energy of the relaxed system, E_{clean} is the total energy of the relaxed clean Cu slab and E_{mol} is the total energy of the adsorbed aromatic molecule calculated in vacuum. Surface distortion energies ($E_{SD} = E_{TSD} - E_{clean}$) and molecular distortion energies ($E_{MD} = E_{TMD} - E_{mol}$) were also calculated, where E_{TSD} is the total energy of the distorted surface and E_{TMD} is the total energy of the distorted molecule. Finally, binding energies are defined as $E_B = E_{ads} - E_{SD} - E_{MD}$.

1. *Naphthalene adsorption sites*

The sites for naphthalene and some of the resulting relaxed adsorption configurations are shown in Figure 5. Table I shows the adsorption energies and the minimum, maximum and average Cu-C distance corresponding to each adsorption site in Figure 5 (a).

In the Table, binding energies E_B of the molecules are also shown. This is a measure of the adsorption energy without the influence of the distortions. Based on this, adsorption site 3 is most favourable, and adsorption site 1, which is best on the total energy, is in third place. The energy difference between all adsorption sites, except site 3, is now smaller than in the case of the original adsorption energies. The adsorption site 8 remains least favourable.

However, at the best adsorption sites the surface underwent considerable distortion. Table I shows that in most cases the distortion energy is negative, indicating that the structural change of the surface is energetically favourable. Figure 6 shows a side and top view of the original surface and the distorted surface from adsorption site 9 where the distortion energy is largest. In all distortion cases the edge row of the longer terrace moves to a new position and causes modification to the whole surface. This effect may be confined to the local environment of a molecule, or alternatively may not happen at all for an isolated molecule. This is because the periodic boundary conditions employed in the calculation imply a reasonably dense Pn film, which could make this reconstruction more favourable than would be the case for an isolated molecule.

For the systems with highest ultimate adsorption energies, the surface distortions have a positive distortion energy. This energy cost is paid via the adsorption of the molecule, which allows the system to ultimately relax into the lowest-energy heavily distorted state. As the lowest Cu layer was fixed in all calculations, the change of the surface structure occurs on four atomic layers. Taking the examples of adsorption sites 8 and 9, which are similar except for that in site 8 no surface distortion occurs, one can see from the table that the difference of the adsorption energies is 0.79 eV which is in this case very significant. However, this value is very near to the difference of the surface distortion energy, which is 0.71 eV. This provides clear evidence that the effect of surface distortion on the adsorption energies is considerable.

We also investigated the charge transfer between molecules and surface using the Bader

						Cu-C distance (Å)			C-C distance (Å)	
site	E_{ads} (eV)	E_{SD}	surface	E_{MD}	E_B	shortest	longest	mean	shortest	longest
1	-1.1	-0.51	distorted	0.09	-0.68	2.25	3.69	2.82	1.38	1.44
2	-0.98	-0.48	distorted	0.20	-0.7	2.24	3.04	2.61	1.40	1.44
3	-0.59	0.16	slightly distorted	0.40	-1.15	2.22	2.44	2.34	1.41	1.45
4	-0.89	-0.43	distorted	0.08	-0.54	2.35	3.21	2.79	1.38	1.44
5	-1.02	0.54	distorted	0.03	-0.51	2.25	3.54	2.98	1.38	1.44
6	-0.98	-0.53	distorted	0.02	-0.42	2.28	3.66	2.95	1.38	1.44
7	-1.09	0.54	distorted	0.12	-0.67	2.25	3.07	2.69	1.38	1.44
8	-0.22	0.16	slightly distorted	0.02	-0.38	2.36	3.23	2.79	1.38	1.44
9	-1.01	-0.55	distorted	0.02	-0.48	2.25	3.71	3.08	1.38	1.44
10	-0.62	-0.04	slightly distorted	0.16	-0.74	–	–	–	–	–
11	-0.18	0.02	slightly distorted	0.01	-0.21	–	–	–	–	–
12	-1.00	-0.47	distorted	0.08	-0.61	–	–	–	–	–
13	-0.43	0.11	slightly distorted	0.08	-0.40	–	–	–	–	–

TABLE I. Table of calculated adsorption energies (E_{ads}), surface distortion energies ($_{SD}$), molecular distortion energies (E_{MD}), binding energies (E_B) and bond lengths for naphthalene adsorption on Fibonacci Cu surface. The numbered sites correspond to those labelled in Figure 5 (a).

charge analysis. The range of charge transfer is $0.25e$ (site 1) to $1.24e$ (site 3) to the surface. Such a charge transfer is significant in the generation of a repulsive electrostatic force between adsorbed molecules, as mentioned above.

We performed some test calculations to investigate the impact of including spin polarisation in the DFT simulations and found no effects. We also calculated the electronic structure with and without spin polarisation on naphthalene adsorption site 1 and found no difference.

In the case of adsorption sites perpendicular to the Cu Fibonacci rows, most of the adsorption energies were much lower than in the cases of adsorption parallel to the rows. Only adsorption site 12 was near the best cases of parallel adsorption sites. Adsorption sites 10, 11 and 13 cause only light distortion to the surface. However, the binding energies are weaker than in the case of parallel adsorption sites.

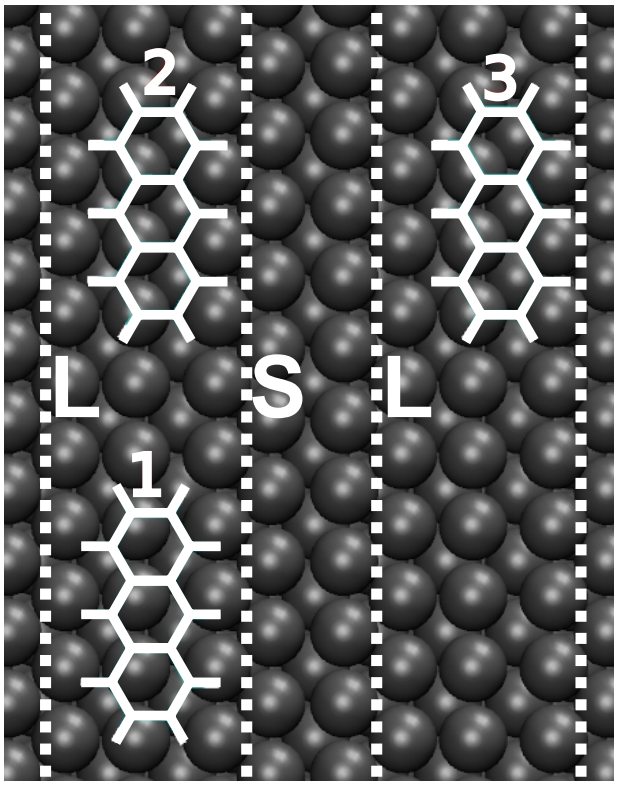

FIG. 7. The starting sites for anthracene adsorption on the Cu/Al-Pd-Mn adsorption system.

2. Anthracene adsorption sites

We studied the adsorption of anthracene on adsorption sites which are parallel to the Fibonacci structure near those sites which proved to be the most favourable in the case of naphthalene (the naphthalene adsorption site number 1). One can see the starting points of relaxation in Figure 7 and the adsorption energies in Table II. Slight differences at the starting point of adsorption made large differences to adsorption energies. For adsorption site 1, no distortion occurs, which also has an affect on the adsorption energy.

If we compare the adsorption energies of the most favourable cases of naphthalene and anthracene by dividing the adsorption energy by the number of C atoms, we can see that they are similar (-0.12 eV/atom in the case of anthracene and -0.11 eV/atom in the case of naphthalene). Therefore, as previously found for adsorption on a simple Pt surface[24], it is possible to approximate adsorption energies of larger aromatic molecules at the same positions as a smaller aromatic molecule. As anthracene has a central ring (as opposed to naphthalene which does not), it is expected to be similar to pentacene in terms of preferred

site	E_{ads} (eV)	surface
1	-0.17	slightly distorted
2	-1.34	distorted
3	-1.70	distorted

TABLE II. Calculated adsorption energies (E_{ads}) for anthracene adsorption on the Fibonacci Cu surface. The numbered sites correspond to those labelled in Figure 7.

adsorption sites.

In addition to the starting structures shown in Figure 7, 8 adsorption sites perpendicular to Cu rows were tried. Early in the calculation, the molecules switched to a parallel orientation. We therefore surmise that perpendicular adsorption will not occur for anthracene adsorption and note that this is consistent with our observations of pentacene adsorption.

Bader analysis of an anthracene in site 1 indicates that there is a charge transfer of $0.58e$ to the surface, which is significant for an electrostatic repulsion between adsorbed molecules as described above.

IV. CONCLUSIONS

We have experimentally investigated the adsorption of Pn on Cu domains with an aperiodic step structure grown on icosahedral Al-Pd-Mn. We have found that Pn molecules do not form islands, rather forming a sparse homogeneous layer, which we interpret in terms of charge transfer between surface and molecules leading to an electrostatic repulsion between adsorbates. We note that certain areas of the Cu film are not covered by Pn molecules up to high Pn coverage (near 1 ML) and observe that this phenomenon is accompanied by a distortion in the surface LDOS of the Cu structure, manifested in variations in apparent height as detected via STM. We demonstrate that the adsorption of Pn at higher coverages leads to an apparently periodic 'checkerboard' structure generated by the adsorption of Pn on alternate Fibonacci rows, driven by the inability to occupy every Fibonacci row due to the flat-lying configuration of the Pn molecules.

To elucidate the fine details of acene adsorption on Fibonacci-modulated Cu, we performed simulations on naphthalene (2 benzene rings) and anthracene (3 benzene rings) adsorbed atop a Cu structure with a local configuration similar to Fibonacci-modulated

Cu. Adsorption energy per C atom is roughly constant, leading to the conclusion that such investigations are useful in predictions of adsorption of higher-order acenes. Additionally, for anthracene, no adsorption site with molecules perpendicular to the Fibonacci structure was stable, consistent with experimental observations of Pn molecules which are universally adsorbed with the molecular long axis parallel to the Fibonacci row structure. We also performed Bader charge decomposition analysis, which indicated charge transfer as a mechanism to understand the repulsive interaction between Pn molecules.

The DFT calculations emphasize the important role that reorganization of the surface Cu atoms plays in aromatic molecular adsorption, as might be expected for the relatively open Fibonacci stepped surface.

V. ACKNOWLEDGMENTS

The EPSRC is thanked for funding under grant number EP/D05253X/1. The Academy of Finland is thanked for funding (projects #218186 and #218546) and CSC-It Center for Science, for computing time.

---

[1] D. Shechtman, I. Blech, D. Gratias, and J. W. Cahn, Phys. Rev. Lett. **53**, 1951 (1984).

[2] R. McGrath, J. A. Smerdon, H. R. Sharma, W. Theis, and J. Ledieu, J. Phys.: Condens. Matter **22**, 084022 (2010).

[3] J. A. Smerdon, J. K. Parle, L. H. Wearing, T. A. Lograsso, A. R. Ross, and R. McGrath, Phys. Rev. B **78**, 075407 (2008).

[4] J. Ledieu, L. Leung, L. H. Wearing, R. McGrath, T. A. Lograsso, D. Wu, and V. Fournée, Phys. Rev. B **77**, 073409 (2008).

[5] J. T. Hoeft, J. Ledieu, S. Haq, T. A. Lograsso, A. R. Ross, and R. McGrath, Phil. Mag. **86**, 869 (2006).

[6] J. Ledieu, C. A. Muryn, G. Thornton, R. D. Diehl, T. A. Lograsso, D. W. Delaney, and R. McGrath, Surf. Sci. **472**, 89 (2001).

[7] E. J. Cox, J. Ledieu, V. R. Dhanak, S. D. Barrett, C. J. Jenks, I. Fisher, and R. McGrath, Surf. Sci. **566-568**, 1200 (2004).

[8] J. A. Smerdon, J. K. Parle, L. H. Wearing, L. Leung, T. A. Lograsso, A. R. Ross, and R. McGrath, J. Phys.: Conf. Ser. **226**, 012006 (2010).

[9] J. A. Smerdon, N. Cross, V. R. Dhanak, H. R. Sharma, T. A. Lograsso, A. R. Ross, and R. McGrath, J. Phys.: Condens. Matter **22**, 345002 (2010).

[10] J. A. Smerdon, L. Leung, J. K. Parle, C. J. Jenks, R. McGrath, V. Fournée, and J. Ledieu, Surf. Sci. **602**, 2496 (2008).

[11] R. McGrath, J. Ledieu, E. J. Cox, S. Haq, R. D. Diehl, C. J. Jenks, I. Fisher, A. R. Ross, and T. A. Lograsso, J. Alloy. Compd. **342**, 432 (2002).

[12] J. Ledieu, J. T. Hoeft, D. E. Reid, J. A. Smerdon, R. D. Diehl, N. Ferralis, T. A. Lograsso, A. R. Ross, and R. McGrath, Phys. Rev. B **72**, 035420 (2005).

[13] J. Ledieu, J. T. Hoeft, D. E. Reid, J. A. Smerdon, R. D. Diehl, T. A. Lograsso, A. R. Ross, and R. McGrath, Phys. Rev. Lett. **92**, 135507 (2004).

[14] K. Pussi, M. Gierer, and R. D. Diehl, J. Phys.: Condens. Matter **21**, 474213 (2009).

[15] K. Lee and J. Yu, Surf. Sci. **589**, 8 (2005).

[16] L. Gavioli, M. Fanetti, M. Sancrotti, and M. G. Betti, Phys. Rev. B **72**, 035458 (2005).

[17] S. Lukas, S. Söhnchen, G. Witte, and C Wöll, ChemPhysChem **5**, 266 (2004).

[18] J. A. Smerdon, M. Bode, N. P. Guisinger, and J. R. Guest, Phys. Rev. B **84**, 165436 (2011).

[19] D. B. Dougherty, W. Jin, W. G. Cullen, J. E. Reutt-Robey, and S. W. Robey, J. Phys. Chem. C **112**, 20334 (2008).

[20] M. Shtein, J. Mapel, J. B. Benziger, and S. R. Forrest, Appl. Phys. Lett. **81**, 268 (2002).

[21] F.-J. Meyer zu Heringdorf, M. C. Reuter, and R. M. Tromp, Nature **412**, 517 (2001).

[22] J. Lagoute, K. Kanisawa, and S. Fölsch, Phys. Rev. B **70**, 245415 (2004).

[23] C. Morin, D. Simon, and P Sautet, J. Phys. Chem. B **108**, 5653 (2004).

[24] C. Morin, D. Simon, and P. Sautet, J. Phys. Chem. B **108**, 12084 (2004).

[25] N. J. Watkins, L. Yan, and Y. Gao, Appl. Phys. Lett. **80**, 4384 (2002).

[26] P. S. Weiss, M. M. Kamna, T. M. Graham, and S. J Stranick, Langmuir **14**, 1284 (1998).

[27] B. Hammer and J. K. Nørskov, Surf. Sci. **343**, 211 (1995).

[28] R. D. Diehl, J. Ledieu, N. Ferralis, A. W. Szmodis, and R. McGrath, J. Phys.: Condens. Matter **15**, R63 (2003).

[29] Z. Papadopolos, G. Kasner, J. Ledieu, E. J. Cox, N. V. Richardson, Q. Chen, R. D. Diehl, T. A. Lograsso, A. R. Ross, and R. McGrath, Phys. Rev. B **66**, 184207 (2002).

[30] W. W. Pai, C.-L. Hsu, M. C. Lin, K. C. Lin, and T. B. Tang, Phys. Rev. B **69**, 125405 (2004).

[31] S. Lukas, G. Witte, and Ch. Wöll, Phys. Rev. Lett. **88**, 028301 (2001).

[32] I. Fernandez-Torrente, S. Monturet, K. J. Franke, J. Fraxedas, N. Lorente, and J. I. Pascual, Phys. Rev. Lett. **99**, 176103 (2007).

[33] J. K. Spong, H. A. Mizes, L. J. LaComb, Jr, M. M. Dovek, J. E. Frommer, and J. S. Foster, Nature **338**, 137 (1989).

[34] G. Kresse and J. Hafner, J. Phys.: Condens. Matter **6**, 8245 (1999).

[35] G. Kresse, and D. Joubert, Phys. Rev. B **59**, 1758 (1999).

[36] P. E. Blöchl, Phys. Rev. B **50**, 17953 (1994).

[37] J. P. Perdew and Y. Wang, Phys. Rev. B **45**, 13244 (1992).